Experimental characterization and methodology for full-wave modeling of ESD to displays

Hossein Rezaei[1], Zhekun Peng[1], Shubhankar Marathe[1], David Pommerenke[2], Cheung Wei Lam[3], Ali Foudazi[3], Daryl Beetner[1], DongHyun Kim[1],

[1]EMC Laboratory, Missouri University of Science and Technology, Rolla, MO 65409, USA
[2]Graz University of Technology, Graz, Austria
[3]Apple Inc. Cupertino, California, USA

***Abstract*— An electrostatic discharge (ESD) to the touchscreen display of a cellphone or other handheld device can result in device failures through sparkless discharge. A test model has been designed and a test board built to investigate sparkless discharge to glass displays, based on the discharge path in a typical product. The current waveform at the touchscreen circuit load was captured during an air discharge using an oscilloscope for 40 test cases with different glass thicknesses, load resistances, and patch-to-ground capacitances. Full wave and circuit models of the discharge event have also been developed. Using the circuit model and a genetic algorithm approach, methods were developed for estimating the input current waveform associated with the discharge event. Using this current waveform, it is possible to predict the magnitude, rise time, total charge, and energy of a typical surface discharges to displays during the early stages of product design to prevent device failures.**

Keywords—Electrostatic discharge, sparkless discharge, genetic algorithm, displacement current, display, modeling, surface discharge.

I. INTRODUCTION

A consistent source of upset or failure in electronic devices is electrostatic discharge (ESD) [1-4]. Discharge to the glass display of a cellphone or other handheld device can be particularly problematic [5, 6]. When a charged object approaches a display, a surface corona discharge will occur. This spark-less discharge can inject currents up to 20 A into the display with pulse lengths of tens of nanoseconds [5, 6]. The surface corona suddenly changes the potential on the glass surface which causes currents on the internal structure due to displacement [5]. These currents on the internal structure can damage or upset touch screens and displays [1-5].

The level of current and waveform depends on the surface capacitance, the resistance and the capacitance of the structure below the glass, as well as other parameters. Thus, thin glass, glass with a high dielectric constant, and low impedance touchscreen circuits are expected to result in larger currents. To estimate early in the design process if a touchscreen will be able to withstand the ESD induced currents, one must be able to simulate these currents and the coupling.

The induced current from spark-less electrostatic discharge events to display screens has been measured in a previous study [5]. In this study, the total current discharged from an ESD gun was captured using an F65 current clamp which was mounted around the air discharge tip [4-7]. The displacement current to patches just beneath the glass was also measured.

In this paper, it is assumed that the failure likelihood is directly related to the energy dissipated to and the peak current in the touchscreen circuit. The ultimate goal of this study, therefore, is to be able to predict possible ESD failures in a new product by predicting the maximum energy dissipated in the touchscreen circuits during an ESD event and by predicting the peak current associated with the event.

Accordingly, this study will focus on the part of the current which flows through the glass to a patch just below the discharge location and which is connected to a touch-screen circuit. A setup was prepared to measure the induced current from an ESD event to the 50 Ω input of an oscilloscope. A full wave model of the setup has been developed, along with a circuit representation. The models represent the coupling path from the front of the touch screen to the load terminating the sensor trace inside the phone [5]. A genetic algorithm (GA) has been developed to find the parts of displacement current which flow through the glass into the display from the induced current measured at the oscilloscope. While displacement current does not truly flow through the glass, it will be referred to that way in the following paper for ease of reference. The current path is depicted in Fig. 1. The GA finds a near-optimal representation of the patch current by iteratively predicting a source current waveform, predicting the current measured at the oscilloscope, then modifying the predicted source current according to the accuracy of the estimated current at the oscilloscope. GA estimates of source currents are found for different glass thicknesses (different glass capacitance, C_{sp}), different touchscreen circuit resistances (R_{load}), and different capacitances between the sensor patch and return structure (C_{pg}).

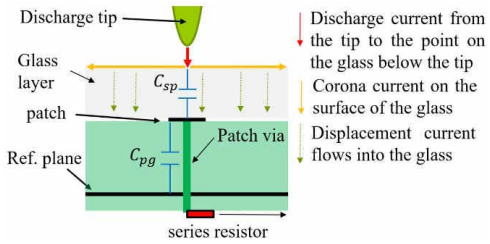

Fig. 1. The spark-less current paths. The ionized surface on glass is modeled as one plate of C_{sp}.

II. MODELING

A. Measurement set-up

As shown in Fig. 1, spark-less current paths are created between the air discharge tip of an ESD generator and the inner structure of the display through surface corona and capacitive coupling. To measure the displacement current that flows through the glass, a measurement setup was prepared inside a climate chamber (Fig. 2). In this setup an ESD gun approaches the glass at a fixed rate [5]. A set of sensor patches are placed just behind the glass and connected through a sensor circuit to the oscilloscope (Fig. 3). It was shown in [5] that a thin air gap between the sensor patches and the glass can influence the discharge current. To prevent any unwanted

effects due to this air gap, a vacuum pump was used to remove air behind the glass. Several test parameters were investigated in [5] including the effect of humidity, approach speed, gun voltage, and polarity. Two PCB boards representing the sensor patches and circuitry were designed and fabricated as shown in Fig. 3. The patches that can be connected to an external resistor acting as a typical load in a touch screen circuit. An oscilloscope is connected in series with this resistor to measure the total load current. Each PCB has 36 2.5 mm by 2.5 mm patches. The two PCB boards were designed to have different capacitive coupling from the patch (top layer) to the ground (bottom layer). This capacitance is about 650 fF and 430 fF for the two PCB boards.

The total current created by the surface corona was previously measured with an F65 current clamp [4, 5, 6] since it was assumed this current was the main factor for the device failure. The partial current which flows through the glass to the internal structure of a specific patch, however, is more likely to be the critical factor that can result in a failure. The waveform for the current which flows to the patch just beneath the discharge was estimated using a genetic algorithm.

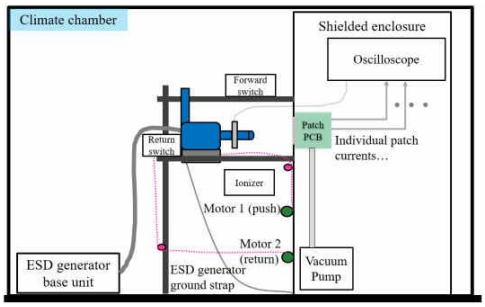

Fig. 2. Measurement setup.

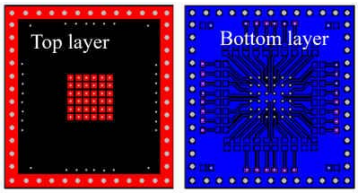

Fig. 3. Top and bottom layer of PCB boards.

B. Full wave simulation model

Full wave and circuit models of the discharge event were developed in CST Studio Suite [8] as shown in Fig. 4. The model includes an excitation source, a 3D model of the glass, sensor patches, and grounding structure. While models of the ESD gun have been used successfully to model electrostatic discharge in other studies [9, 10], coronal discharge is much more complicated and is difficult to model in a full-wave simulation tool. For that reason, the coronal discharge was represented only as a current source to a low ohmic metal disk with a fixed radius as excitation [5], as shown in Figs. 4c and 4d. The current waveform was determined using the GA as shown later in this paper. The excitation source was connected to the return plane with a ground wire, similar to the ground strap used on an ESD gun, as shown in Fig. 4c. While the inductance of the loop formed by this wire causes some voltage on the wire and thus capacitive coupling to other structures, the inductance (about 50 nH) and associated voltage is not large enough to significantly influence results. The excitation is delivered to a small disk on top of the glass and above the patch, which represents a conductive layer created by the coronal discharge [5]. The co-simulation feature of CST Microwave Studio [7] was used to simulate the 3D full-wave model of the setup with a circuit model of the current source.

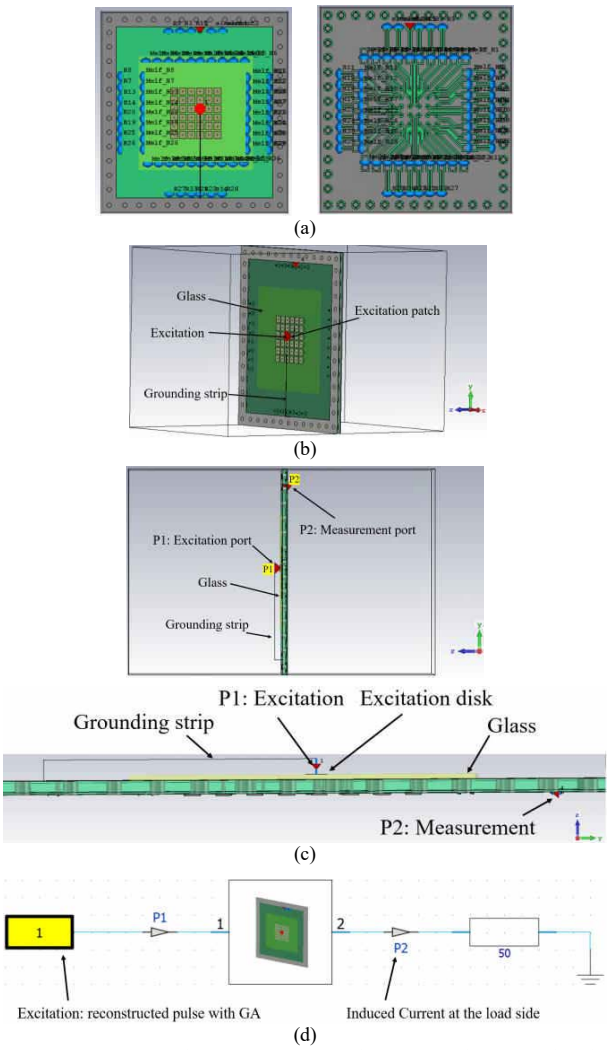

Fig. 4. a) Top and bottom layer of full-wave simulation model, b) Excitation with grounding strip (front view), c) Excitation with grounding strip (side view) e) Display model in CST Microwave Studio with time domain excitation.

C. Circuit model

A simple SPICE model (Fig. 5) was derived from the full-wave model to represent the overall discharge event. The capacitive coupling from the excitation port to the patch (C_{sp}) was found to be 0.65, 0.43, and 0.125 pF for the three glasses studied, which had thicknesses of 0.6, 0.9 and 1.6 mm, respectively. The capacitor C_{pg} represents the capacitive coupling from the patch to the ground plane. The two PCB boards were designed to make this capacitance 0.485pF and 2.9 pF, respectively. Several capacitors were added to these boards to investigate the induced current for products with higher capacitances e.g., 4.7, 15 and 30 pF. The capacitance between the conductive surface created by the corona and ground (C_{sg}) is also considered in Fig. 5b. A problem with the use of C_{sg} is that the conductivity of the corona surface is time dependent and we initially do not know the value of C_{sg}. A method to estimate the size of this capacitor is described in Section E.

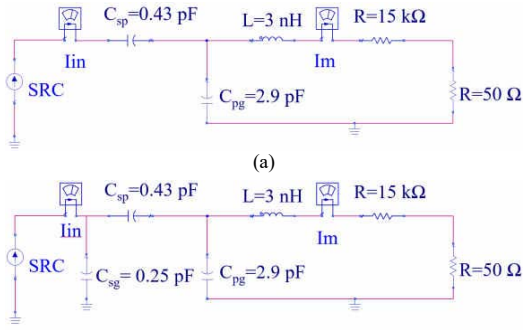

Fig. 5. Schematic of circuit model. a) without coupling from surface to ground (C_{sp}), b) with coupling from surface to ground (C_{sg}).

D. Genetic Algorithm (GA)

The process used to find an appropriate excitation current waveform is shown in Fig. 6. GA was used to tune the excitation current waveform (I_{in}) such that the current resulting in the 50 Ω termination of the patch (I_m) was similar to the current measured with the oscilloscope. The cost function for the GA was tuned to find an input pulse with 0% error in the delivered energy, with up to 30% error in the peak current, and up to 300% error in the rise time. This mix was chosen as an appropriate trade-off between these parameters, with a priority on optimizing the dissipated energy and peak of the current, since these parameters are most likely to lead to failure. The input pulse waveform was constructed using a continuous function which has different fall and rise times:

$$I(t) = I_{High} \times \left[e^{\frac{-(t-Delay1)}{Tau1}} + e^{\frac{(t-Delay1)}{Tau2}} \right]^{-1} \quad (1)$$

where the current source parameters need to be tuned are:

- I_{High} (magnitude)
- Delay1 (time delay)
- Tau1 (Rising edge time constant)
- Tau2 (Falling edge time constant)

The first exponential is related to the LR time constant of the gun and current return path. The second exponential is due to the RC time constant of the gun and surrounding structure [11, 12]. The current at the oscilloscope, I_{in}, can be found by solving a second order ordinary differential equation (ODE) using a dependent variable I_m and independent variable t as:

$$L_1 \frac{d^2 I_m}{dt^2} + (R_1 + R_2) \frac{dI_m}{dt} + \frac{1}{C_2} I_m = \frac{1}{C_2} I_{in} \quad (2)$$

To solve this equation using the Matlab function ode45, (2) has to be converted to a set of first order ODE's. Two new variables X_1 and X_2 are defined as:

$$\begin{cases} X_1 = X \\ X_2 = X' \end{cases} \Rightarrow\Rightarrow \begin{cases} X'_1 = X' \\ X'_2 = X'' \end{cases} \quad (3)$$

Therefore, two new first order ODE equations can be written as:

$$\begin{cases} X'_1 = X_2 \\ X'_2 = \dfrac{-(R_1 + R_2)}{L_1} X' - \dfrac{1}{L_1 C_2} X + \dfrac{1}{L_1 C_2} I_{in} \end{cases} \quad (4)$$

The Matlab code used to solve (4) is [13]:

```
"initial_x    = 0;
initial_dxdt = 0;
[t,x]=ode15s( @rhs, t, [initial_x initial_dxdt] );
function
dxdt = rhs(t,x)
dxdt_1 = x(2);
[I_Source] =AnPulse(I_High,Delay1,Tau1,Delay2,Tau2,t);
 dxdt_2 = -(R1+R2)/L1*x(2) - 1/(L1*C2)*x(1) +
1/(L1*C2)*I_Source;
dxdt=[dxdt_1; dxdt_2];
end"
```

where "AnPulse" is a function which returns the induced current pulse using (1).

The GA attempts to find the input pulse that minimizes the overall relative error in the estimated and measured current at the oscilloscope. The definition of relative error is shown in equations (5)-(7), where RE_1 is the relative error in the energy of the current waveform, RE_2 is the relative error in the rise time, and RE_3 is the relative error in the peak current.

$$RE_1 = \frac{|Energy_{GA} - Energy_{Measured}|}{|Energy_{Measured}|} \quad (5)$$

$$RE_2 = \frac{|Rise\ time_{GA} - Rise\ time_{Measured}|}{|Rise\ time_{Measured}|} \quad (6)$$

$$RE_3 = \frac{|Peak_{GA} - Peak_{Measured}|}{|Peak_{Measured}|} \quad (7)$$

Since the GA must optimize the pulse according to a single error measure, a single measure was formed from a weighted sum of the three relative errors:

$$Total\ Error = \alpha RE_1 + (1 - \alpha) RE_2 + \alpha RE_3 \quad (8)$$

where α is a weighting coefficient that was determined heuristically, based on the authors' observations of several fitted waveforms and the relative importance of fitting for rise time, peak current, and total energy, as will be explained further later in the manuscript.

During each iteration, the GA generates and tests several variations of the waveform parameters shown in (1). The set of parameters at the end of each iteration are "optimal" for that iteration. At the end of the iteration, the relative error produced by this set of parameters is compared to the relative error produced by the last iteration. If the change in relative error is less than or equal to a convergence threshold μ, the simulation is considered to have converged, and will output the optimized pulse. Otherwise, the pulse parameters will be changed, and the GA will be executed again.

Table I summarizes the measured and estimated current waveforms for one test case. The case was measured with a charge voltage of 9 kV, load resistor = 15 kΩ, C_{sp} = 0.43 pF and C_{pg} = 2.9 pF. Three weighting coefficients were tested for the GA approach, α = 0.1, 0.2 and 0.4. The reconstructed input and output currents are shown in Fig. 7 and Fig. 8, respectively. For clear comparison in Fig. 7, the waveforms have been shifted in time, so they do not overlap. Among these trials, it was determined that the selection of 0.4 for the weighting coefficient (GA 03) leads to better waveforms. This coefficient, however, brings less priority to the rise time compared to the pulse energy and peak. Since the rise time is

not quite repeatable in measured ESD event, it was decided to accept even up to 300% error in the rise time as long as the error in energy is almost zero and the peak has less than 30% error.

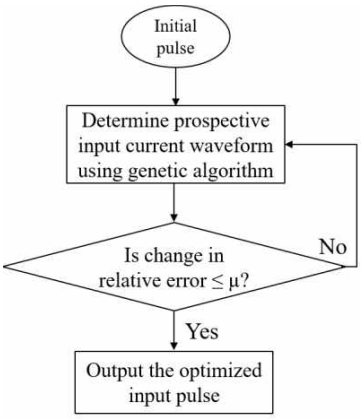

Fig. 6. Process used to find current waveform with the GA method.

TABLE I. SUMMARY COMPARISON BETWEEN MEASURED AND ESTIMATED CURRENT.

	a	*Energy (μJ)*	*Tr (ns)*	*Peak (mA)*	*Iteration*
Target	-	**≈ 2.2**	**≈ 0.47**	**≈ 0.072**	-
GA 01	0.1	≈ 2.2 Error = 0%	≈ 1.9 Error = 304%	≈ 0.076 Error = 5.5%	29
GA 02	0.2	≈ 2.2 Error = 0%	≈ 1.9 Error = 304%	≈ 0.076 Error = 5.5%	12
GA 03	0.4	≈ 2.2 Error = 0%	≈ 1.8 Error = 283%	≈ 0.076 Error = 5.5%	25

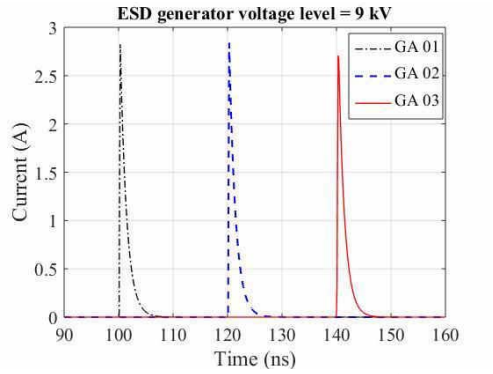

Fig. 7. Reconstrcuted input currents estimated with different weighting coefficients for a 9 kV event. Waveforms have been shifted in time for better visibility.

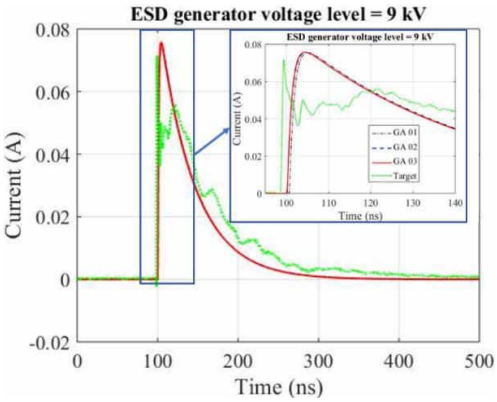

Fig. 8. Reconstrcuted output (induced) currents for different weighting coefficients for a 9 kV event.

E. Compensating current waveform for full-wave simulation

The waveform estimated using GA is based on the circuit in Fig. 5a. Fig. 5a, however, does not include the capacitance C_{sg} between the conductive surface created by the corona and the ground plane under the display. This capacitance reduces the amount of current delivered to the touchscreen circuitry and is present in the full wave simulation model in Fig. 4. Before the GA estimated current waveform can be used in the full wave simulation, the waveform must be compensated to account for the presence of C_{sg}.

Two methods were used to find and compensate for C_{sg}. The first method finds the value of C_{sg} by comparing the impedances found in the full-wave simulation with the impedance found in the circuit shown in Fig. 5b. The S-parameters between the excitation input and the oscilloscope are exported from the full-wave model and are used to estimate the input impedance looking from the excitation source into the glass (Fig. 9). This impedance is compared to the impedance seen looking into the glass in Fig. 5b. The value of C_{sg} in Fig. 5b is iteratively modified until the two impedances are the same. The estimated source current waveform found using the GA is then placed in the circuits shown in Fig. 5a and Fig. 5b to find the oscilloscope output estimated by each circuit. A compensation coefficient is then found, such that when the waveform used in Fig. 5b is multiplied by the compensation coefficient, the output at the oscilloscope is the same for Fig. 5a and Fig. 5b. This compensated waveform may be used in the full-wave model.

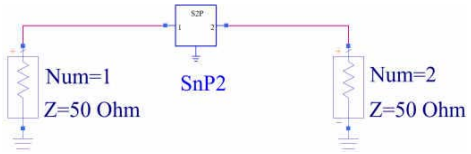

Fig. 9. Circuit schematic in ADS.

The second method uses a similar approach but estimated the value of C_{sg} by comparing the waveform at the oscilloscope as estimated in CST and in Fig. 5b. With this method, the GA estimated waveform is used with the co-simulation tool in CST to estimate the output waveform. The GA estimated waveform is similarly applied to the circuit in Fig. 5b, and the value of C_{sg} in Fig. 5b is modified until this circuit and the CST simulation give the same waveform at the oscilloscope. Once C_{sg} has been found, a compensation coefficient can be found as in the first method, by applying the GA estimated waveform to the circuits in Fig. 5a and Fig. 5b and adjusting the compensation coefficient until the two output waveforms match.

III. DISCUSSION

Tests have been performed for twenty combinations of resistive loads, for different values of C_{pg}, for different glass thickness, and with the ESD generator set to different voltages, i.e. to 9 and 15 kV. These tests were performed to provide more insight into the induced current with different display parameters. Each test was repeated up to 5 times to find the case with the highest energy delivered to the load.

The genetic algorithm was used to tune the excitation current in I_{in} such that the current in the 50 Ω termination of the patch (I_m) is similar to the measurements for all test cases. The effect of having different glass thickness, load resistor and

the capacitive coupling from patch to ground will be discussed in the following sections.

A. Compensation Coefficient

As discussed earlier, the corona creates a more or less conductive surface which creates the capacitance C_{sg} between the corona surface and the ground plane. A problem with the use of C_{sg} is that the conductivity of the corona surface is time dependent. The value of C_{sg} estimated for the test cases was about 0.25 pF. Based on this value, a compensation coefficient of 1.6 is suggested when using the GA estimated waveform in the full-wave model or in Fig. 5b. This coefficient should be multiplied with the input current source estimate by GA.

B. Effect of Glass Thickness and Dielectric Constant

One of the main factors in the display industry is the glass thickness. The glass is mounted between the excitation and the patch in Fig. 4. Three different glasses of the same type were used to investigate the effect of glass thickness on peak value and energy in the induced current. Table II shows the current waveform characteristics for glass that is 0.6, 0.9, and 1.6 mm thick when the ESD gun was charged to 9 and 15 kV. The peak discharge current and total dissipated energy increases for thinner glass thickness. The glass with 0.6 mm thickness has the highest total energy and peak current.

The glass capacitance C_{sp} in Fig. 5 was estimated to be 0.125, 0.43 and 0.65 pF for glass thicknesses of 1.6, 0.9 and 0.6 mm, respectively. The higher the capacitance, the higher the induced current and total energy. The higher current and energy might be explained by a stronger surface ionization for thinner glass [5]. The results show that the risk of upset or failure from spark-less discharge increases for thinner glass thickness.

TABLE II. MEASURED CURRENT WAVEFORM CHARACTERISTICS FOR DIFFERENT GLASS THICKNESSES.

	9 kV			*15 kV*		
Thickness (mm)	$I_{in,peak}$ ***(A)***	$I_{out,peak}$ ***(A)***	***Energy (μJ)***	$I_{in,peak}$ ***(A)***	$I_{out,peak}$ ***(A)***	***Energy (μJ)***
1.6	0.4	0.02	0.062	0.8	0.032	0.21
0.9	2.5	0.1	2.3	4.5	0.17	5.56
0.6	2	0.14	4.1	5.5	0.2	10

C. Effect of Load Resistor and Capacitor

Other factors which contribute to the level of current during a spark-less discharge is the value of the resistive load and the capacitance of patch to ground (C_{pg}). The resistive load (R = 15 kΩ in Fig. 5) is defined by the product. Fig. 10 shows the reconstructed input currents using GA for a 9 kV discharge for different loads and Fig. 11 shows the resulting output current I_m. For clear representation in Fig. 10, waveforms have been shifted in time by 20 ns (blue curve, R = 10 kΩ) and 40 ns (red curve, R = 15 kΩ). While the input currents are similar for the three loads, the induced/output current (I_m) is lower for higher resistor value (Fig. 11) because the high resistance forces more current to return through C_{pg}. The total energy dissipated by the larger resistors is higher than the smaller resistors even with lower induced current, due to the higher time constant of the current waveform associated with the larger resistor.

The voltage on the excitation disk during the discharge event is shown in Fig. 12 for three different loads. The input voltage is higher for higher loads. The small overshoot above the ESD gun voltage of 9 kV for 10 and 15 kΩ loads is due to the roughly 10% error in the peak value of the reconstructed current. For 380 Ω, the duration of induced current is very short which correspond to a large dI/dt. This could create thermal damage that is harmful to the DUT, possibly even worse than other loads [14].

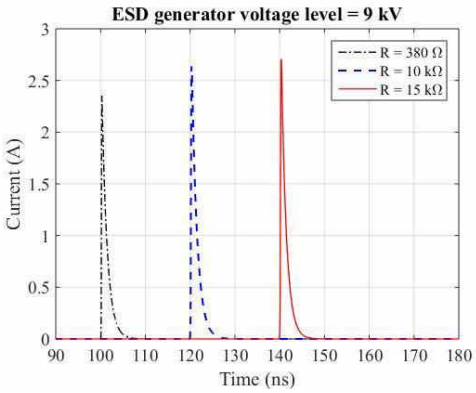

Fig. 10. Reconstrcuted input currents (I_{in} in Fig. 10) for different loads with a 9 kV discharge level. Waveforms have been shifted in time for better visibility. (C_{sp} = 0.43 pF, C_{pg} = 2.9 pF)

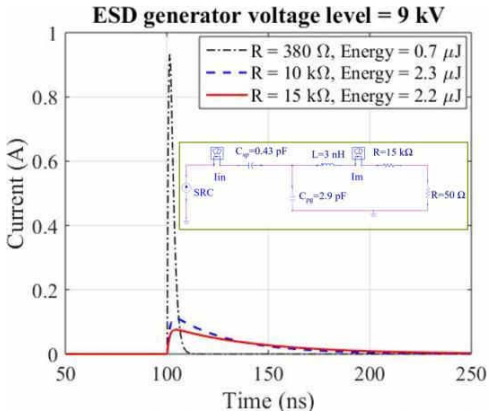

Fig. 11. Reconstrcuted induced (output) currents (I_m) for different loads with a 9 kV discharge level.

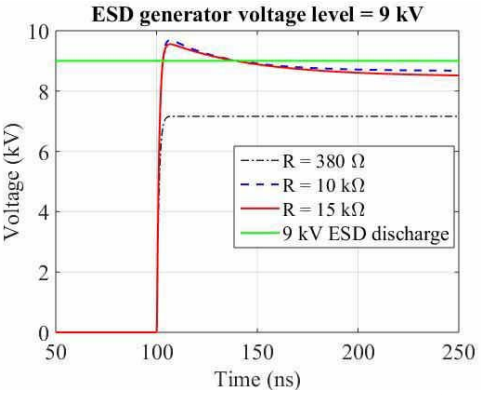

Fig. 12. Reconstrcuted input voltage on the center patch for different loads with a 9 kV discharge level.

Fig. 13 shows the effect of having a higher C_{pg} on the input current, I_{in}, and Fig. 14 shows the associated waveform at the output, I_m. The currents were measured with a discharge voltage of 9 kV. The higher the value of C_{pg}, the lower the peak current and the energy in both the input and output waveforms. This result suggests that thinner boards for the display circuits should be used, creating a smaller gap between the patch and ground and a higher C_{pg}. For the tests conducted here, one board has a 0.8 mm distance between the patch and

ground giving C_{pg} = 2.9 pF. For the second board, however, the distance is about 1.6 mm and C_{pg} = 0.485 pF. The decrease in the current with C_{pg} might be explained by a weaker channel ionization, and an associated smaller discharge current. this result indicates that the ever further reduction of PCB board thicknesses may decrease the risk of upset or failure by sparkless discharges.

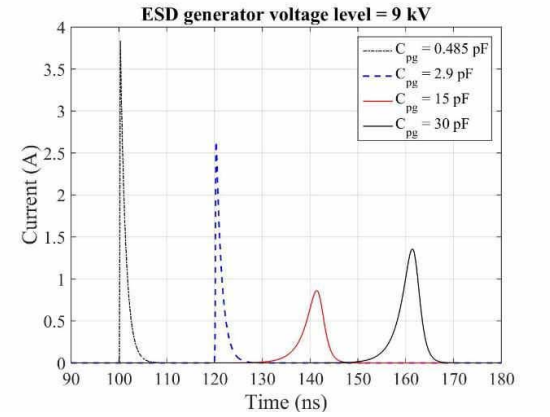

Fig. 13. Reconstrcuted input currents (I_{in}) for different values of C_{pg} with a 9 kV discharge level. Waveforms have been shifted in time for better visibility.

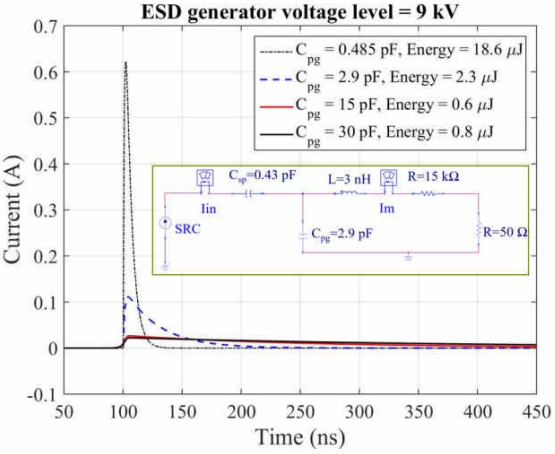

Fig. 14. Reconstrcuted induced currents (I_m) for different values of C_{pg} with a 9 kV discharge level.

IV. Conclusion

A test model was developed to study sparkless discharge to touchscreen displays. The air discharge event was captured with an oscilloscope for 20 test cases having different glass thickness, load resistance, and load capacitance. Full-wave and circuit models representing the sparkless discharge were developed and were validated with measurements. Further, a GA approach was used to estimate a source current waveform representing the parts of the displacement current which flows through the glass into the patch just below the discharge event. The current waveform was estimated from the current measured at the circuit load with an oscilloscope and using a circuit representation of the discharge event. Using the GA estimated current waveform and the circuit model, it is possible to predict the peak current and total energy dissipated in the touch layer during the pre-design phase of a new product without performing new measurements. In future studies, the discharge event will be further characterized based on the test model's parameters e.g., glass thickness, load resistance and load capacitance.

Acknowledgment

This paper is based upon work supported partially by the National Science Foundation (NSF) under Grants IIP-1916535.

References

[1] J. Ko, K. Kim, and H. Kim, "System-level ESD immunity of mobile display driver IC to hard and soft failure," Elect. Electron. Eng., vol. 13, no. 1, pp. 329-335, 2012.

[2] K.Kim andY.Kim, "Systematic analysis methodology for mobile phone's electrostatic discharge soft failure," IEEE Trans. Electromagn. Compat., vol. 53, no. 3, pp. 611-618, Aug. 2011.

[3] H. Rezaei, L. Guan, A. Talebzadeh, S. Marathe, P. Wei, D. Pommerenke, "Effect of Relative Humidity and Materials on Triboelectric Charging of USB Cables," IEEE International Symposium on Electromagnetic Compatibility & Signal/Power Integrity (EMCSI), pp. 634-639, Aug. 2017.

[4] S. Marathe, H. Rezaei, D. Pommerenke, M. Hertz, "Detection Methods for Secondary ESD Discharge During IEC 61000-4-2 Testing," IEEE International Symposium on Electromagnetic Compatibility & Signal/Power Integrity (EMCSI), pp. 152-157, Aug. 2017.

[5] Y. Gan, A. Talebzadeh, X. Xu, S. Shinde, Y. Zeng, K.-H. Kim, and D. Pommerenke, "Experimental Characterization and Modeling of Surface Discharging for an Electrostatic Discharge (ESD) to an LCD Display," IEEE Transactions on Electromagnetic Compatibility, Vol. 60, No. 1, pp. 96-106, Feb. 2018.

[6] S. Marathe, G. Maghlakelidze, H. Rezaei, D. Pommerenke, and M. Hertz, "Software-Assisted Detection Methods for Secondary ESD Discharge During IEC 61000-4-2 Testing," IEEE Trans. Electromagn. Compat., vol. 60, no. 4, pp. 1129-1136, Aug. 2018.

[7] S. Marathe, D. Li, A. Hosseinbeig, H. Rezaei, P. Wei, J. Zhou, D. Pommerenke, "On Secondary ESD Event Monitoring and Full-wave Modeling Methodology," 39th Electrical Overstress/Electrostatic Discharge Symposium (EOS/ESD), Sep. 2017.

[8] Available online at: https://www.3ds.com/productsservices/simulia/products/cst-studio-suite/solvers/

[9] J. Xiao et al., "Model for ESD LCD upset of a portable product," in Proc. IEEE Int. Symp. Electromagn. Compat., 2010, pp. 354-358.

[10] J. Xiao et al., "Model of secondary ESD for a portable electronic product," IEEE Trans. Electromagn. Compat., vol. 54, no. 3, pp. 546-555, Jun. 2012.

[11] F. Asimakopoulou, G.P. Fotis, I.F. Gonos, I.A. Stathopulos, "Parameter Determination of Heidler's Equation for the ESD Current", in Proc., 15th International Symposium on High-Voltage Engineering (ISH 2007) , Ljubljana, Slovenia, 2007, paper T2-208.

[12] K. Wang, D. Pommerenke, R. Chundru, T. V. doren, J. L. Drewniak, A. Shashindranath, "Numerical modeling of electrostatic discharge generators," IEEE Transactions on Electromagnetic Compatibility, vol. 45, no 2, pp. 258-270, May 2003.

[13] Available online at: https://www.mathworks.com/matlabcentral/answers/268728-solve-a-system-of-differential-equations-using-ode-45.

[14] M. Mardiguian, "Electrostatic Discharge". IEEE 2009.